

Interleukin-6-deficient mice develop hepatic inflammation and systemic insulin resistance

V. B. Matthews · T. L. Allen · S. Risis · M. H. S. Chan · D. C. Henstridge · N. Watson · L. A. Zaffino · J. R. Babb · J. Boon · P. J. Meikle · J. B. Jowett · M. J. Watt · J.-O. Jansson · C. R. Bruce · M. A. Febbraio

Received: 29 March 2010 / Accepted: 7 July 2010 / Published online: 11 August 2010
© Springer-Verlag 2010

Abstract

Aims/hypothesis The role of IL-6 in the development of obesity and hepatic insulin resistance is unclear and still the subject of controversy. We aimed to determine whether global deletion of *Il6* in mice (*Il6*^{-/-}) results in standard chow-induced and high-fat diet (HFD)-induced obesity, hepatosteatosis, inflammation and insulin resistance.

Methods Male, 8-week-old *Il6*^{-/-} and littermate control mice were fed a standard chow or HFD for 12 weeks and phenotyped accordingly.

Results *Il6*^{-/-} mice displayed obesity, hepatosteatosis, liver inflammation and insulin resistance when compared with control mice on a standard chow diet. When fed a HFD, the *Il6*^{-/-} and control mice had marked, equivalent gains in

body weight, fat mass and ectopic lipid deposition in the liver relative to chow-fed animals. Despite this normalisation, the greater liver inflammation, damage and insulin resistance observed in chow-fed *Il6*^{-/-} mice relative to control persisted when both were fed the HFD. Microarray analysis from livers of mice fed a HFD revealed that genes associated with oxidative phosphorylation, the electron transport chain and tricarboxylic acid cycle were uniformly decreased in *Il6*^{-/-} relative to control mice. This coincided with reduced maximal activity of the mitochondrial enzyme β -hydroxyacyl-CoA-dehydrogenase and decreased levels of mitochondrial respiratory chain proteins.

Conclusions/interpretation Our data suggest that IL-6 deficiency exacerbates HFD-induced hepatic insulin resistance and inflammation, a process that appears to be related to defects in mitochondrial metabolism.

Electronic supplementary material The online version of this article (doi:10.1007/s00125-010-1865-y) contains supplementary material, which is available to authorised users.

V. B. Matthews · T. L. Allen · S. Risis · M. H. S. Chan · D. C. Henstridge · N. Watson · L. A. Zaffino · J. R. Babb · P. J. Meikle · J. B. Jowett · C. R. Bruce · M. A. Febbraio (✉)
Cellular and Molecular Metabolism Laboratory,
Baker IDI Heart & Diabetes Institute,
PO Box 6492, St Kilda Road Central,
Melbourne 3008, VIC, Australia
e-mail: mark.febrario@bakeridi.edu.au

J. Boon · M. J. Watt
Department of Physiology, Monash University,
Clayton, VIC, Australia

J.-O. Jansson
Institute of Neuroscience and Physiology/Endocrinology,
Sahlgrenska Academy, University of Gothenburg,
Gothenburg, Sweden

Keywords Cytokines · Fatty liver · Obesity · Signal transduction · Type 2 diabetes

Abbreviations

| | |
|--------------|--|
| ALT | Alanine transaminase |
| AMREP | Alfred Medical Research and Education Precinct |
| GSEA | Gene Set Enrichment Analyses |
| GTT | Glucose tolerance test |
| β -HAD | β -Hydroxyacyl-CoA-dehydrogenase |
| HFD | High-fat diet |
| IKK | Inhibitor of kappa kinase |
| ITT | Insulin tolerance test |
| JNK | c-Jun N-terminal kinase |
| PKC | Protein kinase C |
| $\dot{V}O_2$ | Oxygen consumption rate |

Introduction

In the past 15 years it has become apparent that obesity is linked to a state of chronic inflammation in tissues such as liver, adipose tissue and skeletal muscle. Obesity results, as reviewed by Hotamisligil [1], in the recruitment of immune cells into adipose tissue beds, where they secrete inflammatory cytokines such as TNF- α . These pro-inflammatory cytokines can, in turn, act via transmembrane receptors to phosphorylate serine/threonine kinases, which are known to disrupt insulin signal transduction [1]. Given this pro-inflammatory response and the observation that systemic IL-6 concentrations are elevated in obesity and patients with type 2 diabetes [2], it is generally accepted that IL-6 contributes to obesity-induced insulin resistance [3]. However, the discovery that IL-6 can be produced and released from skeletal muscle during exercise, led many investigators, as reviewed by Pedersen and Febbraio [4], to challenge this concept because insulin action is enhanced in the immediate post-exercise period.

Presently, the role of IL-6 in insulin resistance is unclear and still the subject of debate [4]. In vitro and ex vivo, acute IL-6 treatment can enhance glucose uptake and fat oxidation [5–9] in skeletal muscle, principally via activation of AMP-activated protein kinase [7]. Acute IL-6 administration during a euglycaemic–hyperinsulinaemic clamp results in a glucose infusion rate that is either unchanged in rats [10, 11], decreased in mice [12] or increased in humans [7]. Short-term (5 to 14 days), exogenous administration of IL-6 to lean rodents causes hepatic insulin resistance in mice [13], but increased whole-body insulin sensitivity and glucose tolerance in rats [14]. Recently, another team has demonstrated that human *IL6* transgenic mice with sustained elevated circulating IL-6 display enhanced central leptin action and improved nutrient homeostasis leading to protection from diet-induced obesity [15].

While initial studies demonstrated that *Il6* knockout (*Il6*^{-/-}) mice display mature-onset obesity [16], subsequent studies did not verify this phenotype [17]. It is also unclear whether these mice display insulin resistance. In the present study, we aimed to determine whether global deletion of *Il6* in mice (*Il6*^{-/-}) results in high-fat diet (HFD)-induced obesity, hepatosteatosis, inflammation and insulin resistance. We show that *Il6*^{-/-} mice develop obesity and insulin resistance, a phenotype associated principally with ectopic lipid deposition and inflammation in the liver. Moreover, when challenged with HFD, *Il6*^{-/-} mice display insulin resistance relative to littermates, despite equivalent adiposity and liver lipid content, demonstrating that IL-6 is necessary to protect against the progression of diet-induced hepatic insulin resistance.

Methods

Animals and diets *Il6*^{-/-} mice were generated by Kopf et al. [18] and backcrossed on to a C57BL/6 background at least nine times to reduce genetic heterogeneity. All experiments were approved by the Alfred Medical Research and Education Precinct (AMREP) Animal Ethics Committee. After a colony was established in the AMREP Precinct Animal Centre under specific pathogen-free conditions, heterozygous breeding pairs were established, and *Il6*^{-/-} and *Il6*^{+/+} animals from the same litters were used in all circumstances. Verification of genotype was determined by PCR (Electronic supplementary material [ESM] Fig. 1) using primers reported previously [17] and by measuring serum IL-6, which was undetectable in *Il6*^{-/-} mice, but averaged 6.0 \pm 3.0 pg/ml in *Il6*^{+/+} mice. Male mice were maintained on a standard chow diet (14.3 MJ/kg, 76% of energy from carbohydrate, 5% from fat, 19% from protein; Specialty Feeds, Glen Forrest, WA, Australia) until 8 weeks of age. At this point, 50% of the animals were switched to a HFD (19 MJ/kg, 35% of energy from carbohydrate, 42% from fat, 23% from protein; Specialty Feeds) for a further 12 weeks.

Body composition, adiposity and indirect calorimetry Body composition was determined via nuclear magnetic resonance imaging (EchoMRI 4-in-1; Echo Medical Systems, Houston, TX, USA) according to manufacturer's instructions. Epididymal adipose tissue was dissected and fixed in 4% paraformaldehyde (wt/wt) overnight before being incubated in 50% ethanol (vol./vol.) and then promptly embedded with paraffin. Adipose tissue was cut into 4 μ m sections and stained with haematoxylin and eosin. For each mouse, ten random fields were photographed. Adipocyte size and number were calculated using Image Pro Plus (Media Cybernetics, Bethesda, MD, USA). Oxygen consumption rate ($\dot{V}O_2$), and respiratory exchange ratio and activity were measured using a twelve-chamber indirect calorimeter (Oxymax; Columbus Instruments, Columbus, OH, USA). Mice had free access to food and water while in the chambers. Food intake was measured manually over a 7 day period, as well as for the duration of data collection while mice were undergoing indirect calorimetry measurements.

Metabolic assays Intraperitoneal glucose tolerance test (GTT) and insulin tolerance test (ITT) were performed in overnight fasted mice. Blood samples were obtained from the tail tip at the indicated times and glucose levels were measured using a glucometer (AccuCheck II; Roche, Castle Hill, NSW, Australia). The doses used during these tests were 1 g/kg lean body mass and 0.5 U/kg lean body mass for GTT and ITT respectively. The homeostatic model assessment of insulin resistance (HOMA-IR) was determined for each animal (equation obtained from www.dtu.ox.ac.uk). Blood samples

were measured for insulin and leptin using standard ELISA kits as previously described [19]. Serum alanine transaminase (ALT) was measured using a standard biochemical assay (Alfred Pathology Services, Alfred Hospital, Melbourne, VIC, Australia). Viral serology, bacteriology and parasitology tests on the mice were performed by The Animal Resource Centre (Murdoch, WA, Australia).

Lipid analysis Plasma and faecal NEFA were analysed according to methods previously described [20]; liver and muscle lipids were analysed as outlined in **ESM Methods**.

Determination of gene expression, protein and enzyme activity Microarray analyses, were performed using a microarray platform (iScan; Illumina, San Diego, CA, USA), with mouse whole-genome gene expression chips (WG-6 version 2.0; 45,281 transcripts). Gene Set Enrichment Analyses (GSEA) was performed using GSEA software (www.broad.mit.edu/gsea/, accessed 1 July 2009) described in detail elsewhere [21, 22]. Real-time RT-PCR was determined as previously described [20]. Proteins were analysed by SDS-PAGE and immunoblotting [20, 23], using primary antibodies from Cell Signaling Technology (Danvers, MA USA), except for the western blotting antibody cocktail for total oxidative phosphorylation, which was obtained from MitoSciences (Eugene, OR, USA). For insulin signalling experiments, mice were anaesthetised with sodium pentobarbital (0.05 mg/g) before a portion of liver and skeletal muscle were excised and snap-frozen in liquid nitrogen. Thereafter, an injection of insulin (1.5 U/kg) was injected into the vena cava and further liver and muscle samples were obtained within 5 min of injection. Liver citrate synthase and β -hydroxyacyl-CoA-dehydrogenase (β -HAD)

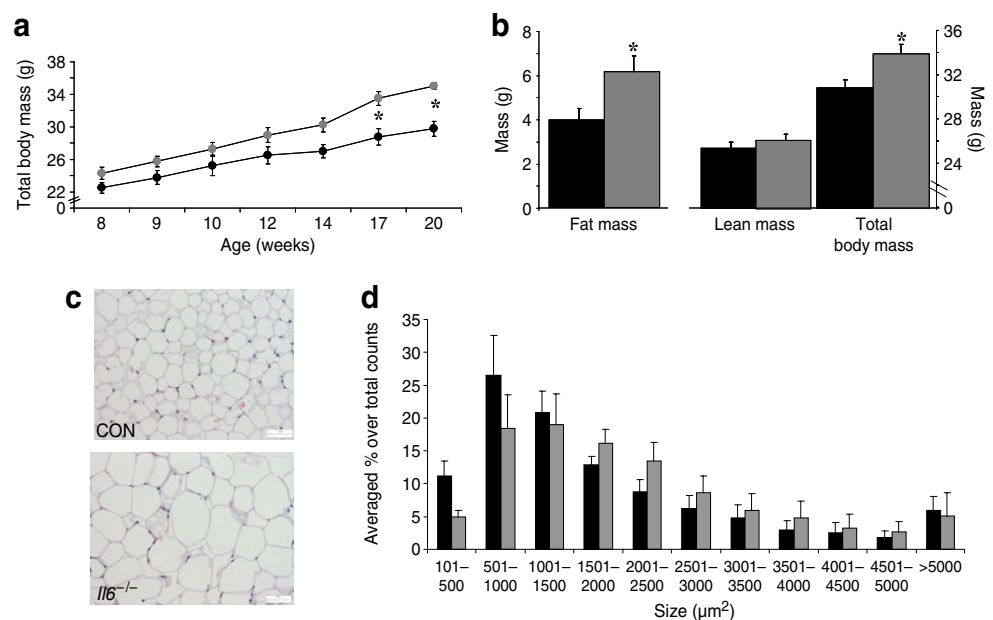
were assayed spectrophotometrically as previously described [23].

Statistical analyses Results are expressed as the mean \pm SEM. Data were analysed for differences by analysis of variance, with specific differences located with a Student–Newman–Keuls post hoc test, or by a Student's *t* test for unpaired samples where appropriate. $p < 0.05$ was considered to be statistically significant.

Results

***Il6*^{-/-} mice become obese at 4 months of age due to increased adipocyte size** It is not clear whether *Il6*^{-/-} mice develop mature-onset obesity [16, 17]. We demonstrated that *Il6*^{-/-} mice developed increased body mass relative to littermate control mice between the ages of 14 and 17 weeks (Fig. 1a). At 20 weeks of age, the *Il6*^{-/-} mice had significantly increased fat mass and total body mass, but comparable lean body mass relative to control (Fig. 1b). The increase in adiposity and total body mass was not associated with alterations in food intake or any observable decreases in activity or whole-body $\dot{V}O_2$ (ESM Table 1). To determine whether the increase in adipose tissue mass was due to increased adipocyte cell size and/or number, we quantified both and also measured the expression of key genes associated with adipogenesis in white adipose tissue. *Il6*^{-/-} mice displayed fat cell hypertrophy with no increase in total cell number relative to control (Fig. 1c, d). In addition, the expression of *Pparg*, *Cebpa* (also known as *Cebpa*) and *Fabp4* in white adipose tissue was not different when comparing *Il6*^{-/-} with control mice (ESM Table 2).

Fig. 1 *Il6*^{-/-} mice develop obesity. Total body mass (a), fat mass, lean mass and total body mass (b), representative tissue cross sections (c) and quantification (d) of adipocyte size from epididymal adipose tissue beds from *Il6*^{-/-} and control (CON) mice. Black bars and/or circles, control; grey bars and/or circles, *Il6*^{-/-}. Measures were made at 20 weeks of age (b–d), when mice were maintained on a standard chow diet. Data expressed as mean \pm SEM, $n = 4$ per group (a), $n = 12$ –17 animals per group for (b), $n = 10$ independent fields from three to five animals for (d); * $p < 0.05$ for difference



Il6^{-/-} mice develop insulin resistance and display marked increases in lipid accumulation and inflammation in the liver. We next examined whether the increase in fat mass in *Il6*^{-/-} mice was associated with insulin resistance and ectopic lipid accumulation in liver and skeletal muscle. At 20 weeks of age, *Il6*^{-/-} mice displayed fasting hyperleptinaemia (Fig. 2a), hyperinsulinaemia (Fig. 2b) and insulin resistance as measured by the HOMA of insulin resistance (Fig. 2c). We next metabolically challenged the mice by performing intraperitoneal ITT and GTT. Compared with control, *Il6*^{-/-} mice displayed marked insulin (Fig. 2d, e) and glucose (Fig. 2f, g) intolerance.

Since hyperlipidaemia and ectopic lipid accumulation are a hallmark of obesity and known to mediate insulin resistance via various signal transduction pathways, we comprehensively examined lipid levels in the mice. Circulating NEFA were not different when comparing strains (data not shown). We next measured lipid species in the liver via thin layer chromatography. Diacylglycerol, but not ceramide was elevated in the livers of *Il6*^{-/-} mice compared with control (ESM Fig. 2a). Thereafter, we adopted a comprehensive lipidomic analysis in the livers and quadriceps skeletal muscle of mice using mass spectrometry. We demonstrated that several triacylglycerol and diacylglycerol species, particularly those containing saturated fatty acids such as palmitate (16:0) and stearate

(18:0), and the monounsaturated fatty acid oleate (18:1), were markedly elevated in the liver (Fig. 3a, b) and skeletal muscle (ESM Fig. 3a, b) of *Il6*^{-/-} mice relative to control. Consistent with our thin layer chromatography analyses, ceramide species did not differ in either tissue when comparing *Il6*^{-/-} with control mice (ESM Fig. 2b, c). Excess lipid accumulation, in particular saturated fatty acids such as palmitate and stearate, is known to activate inflammatory signalling pathways leading to impaired insulin signal transduction [24]. Accordingly, we next measured markers of inflammation and insulin signalling in liver and skeletal muscle of *Il6*^{-/-} and control mice. ALT, a liver enzyme released into the circulation during liver injury, was elevated in the plasma of *Il6*^{-/-} mice relative to control (Fig. 4a). Both inhibitor of kappa kinase (IKK) [25] and c-Jun N-terminal kinase (JNK) [26] are molecules central to inflammatory signalling that are implicated in dysregulation of insulin signal transduction. Total and phosphorylated JNK were elevated in the liver (Fig. 4b), while IKK phosphorylation tended to be elevated in the liver (Fig. 4c), but was significantly higher in the skeletal muscle (ESM Fig. 3c) of *Il6*^{-/-} mice relative to control. In contrast, there was no difference in JNK in skeletal muscle between the strains of mice (data not shown). We next measured *Tnf-α* (also known as *Tnf*) mRNA and TNF-α protein levels in the liver. While neither *Tnf-α* mRNA

Fig. 2 *Il6*^{-/-} mice exhibit insulin resistance. Leptin (a), insulin (b), HOMA of insulin resistance (HOMA-IR) (c), insulin tolerance (d) with corresponding AUC (e) and (f) glucose tolerance with AUC (g) in *Il6*^{-/-} and control mice. Black bars and/or circles, control (CON); grey bars and/or circles, *Il6*^{-/-}. Measures were made at 20 weeks of age, when mice were maintained on a standard chow diet. Data expressed as mean ± SEM, *n*=12–17 animals per group; **p*<0.05 for difference

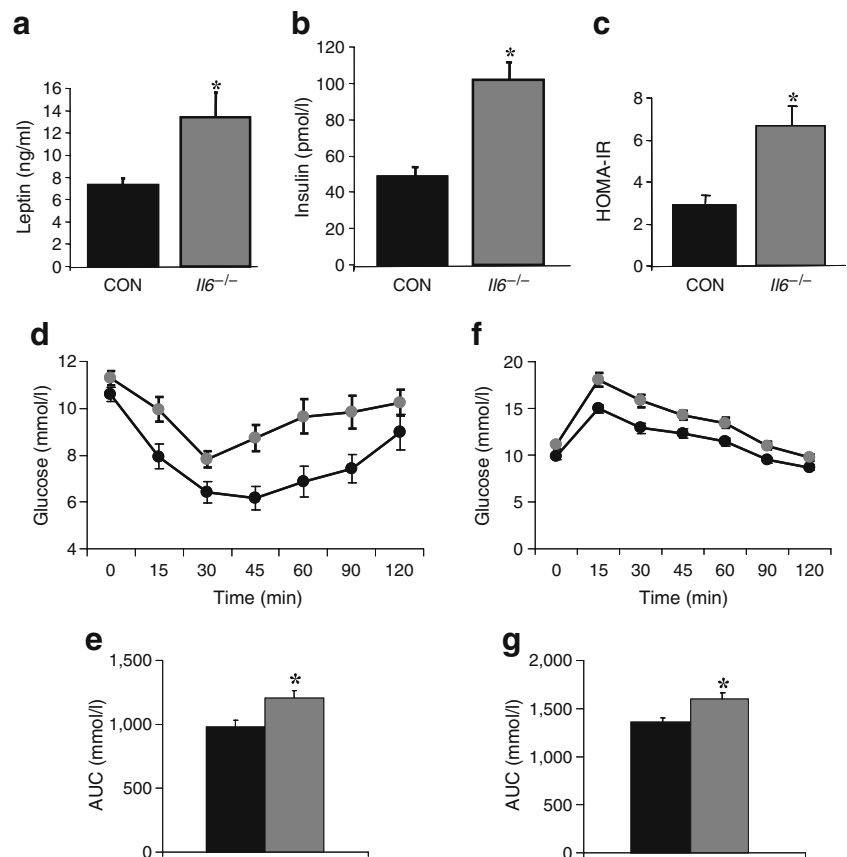
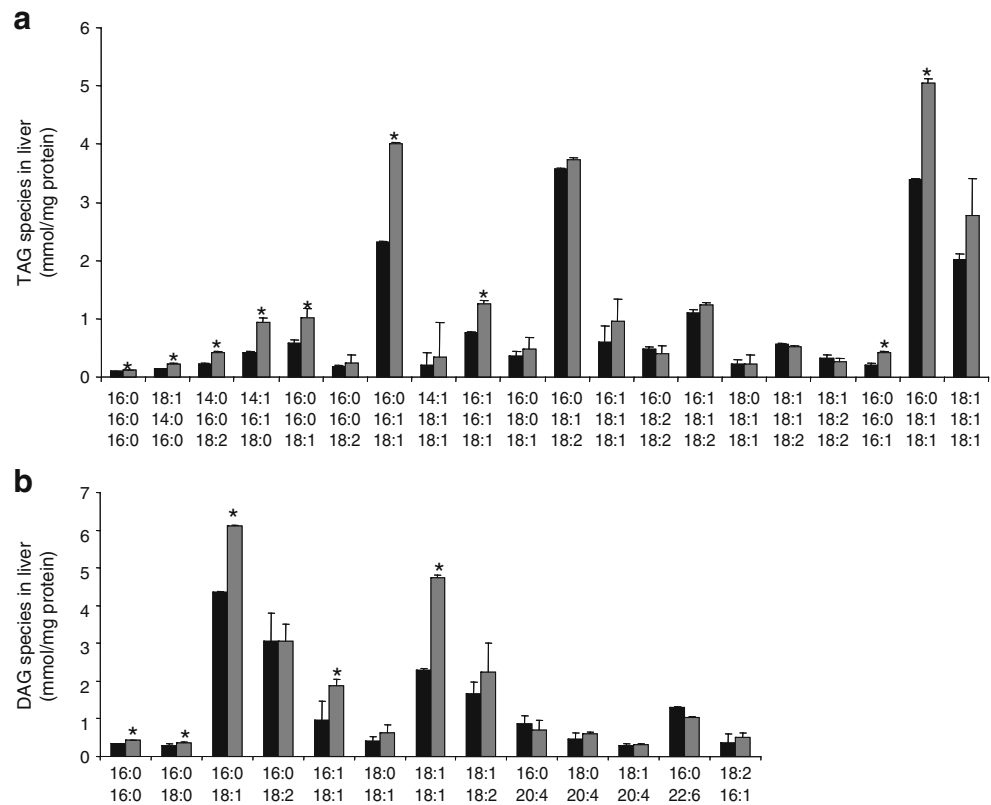


Fig. 3 *Il6*^{-/-} mice develop hepato-steatosis. **a** Liver triacylglycerol (TAG) and **b** diacylglycerol (DAG) species in liver samples obtained from control (black bars) and *Il6*^{-/-} (grey bars) mice at 20 weeks of age maintained on a standard chow diet. Data expressed as mean \pm SEM, $n=8$ animals per group; * $p<0.05$ for difference

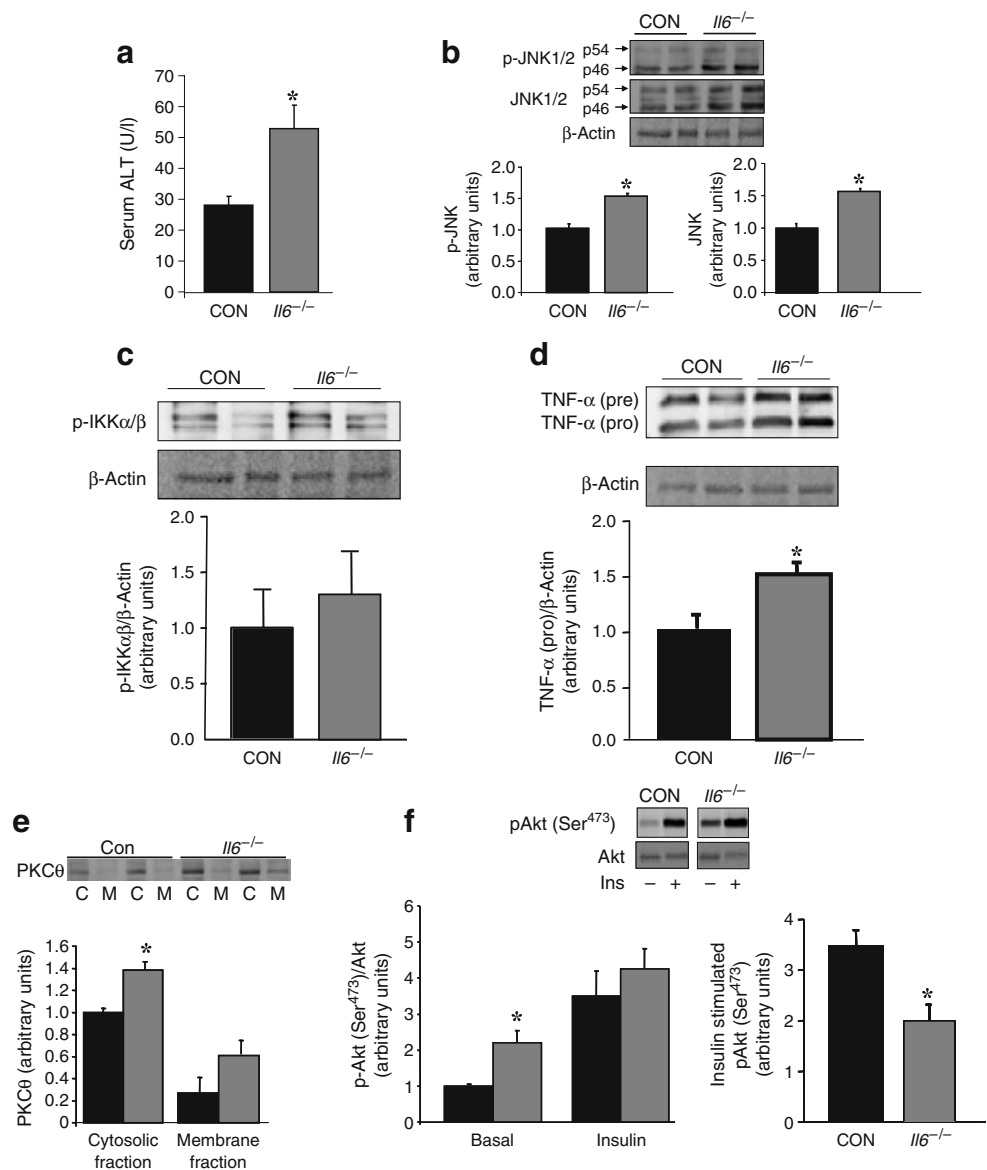


abundance (data not shown) nor pre-(cytosolic) TNF- α protein levels (Fig. 4d) were different when comparing strains, pro-(membrane bound) TNF- α protein was increased in the livers of *Il6*^{-/-} mice compared with control (Fig. 4d).

Diacylglycerol is known to act as a second messenger for many signal transduction pathways, including the novel protein kinase C (PKC) family. PKC δ [27] and PKC θ [28] have been implicated in diacylglycerol-induced insulin resistance. Accordingly, we measured levels of these proteins in the liver and skeletal muscle of *Il6*^{-/-} and control mice. While there were no differences in the levels of PKC δ in the liver when comparing strains (data not shown), we observed an increase in the cytosolic fraction and a tendency ($p=0.05$) for an increase for PKC θ in the membrane fraction in liver of *Il6*^{-/-} mice (Fig. 4e). However, no differences were detected when comparing strains for both PKC isoforms in skeletal muscle (data not shown), despite the increased diacylglycerol accumulation in this tissue. Phosphorylation (Ser⁴⁷³) of Akt was increased when comparing *Il6*^{-/-} with control mice in the basal state (absence of insulin stimulation) (Fig. 4f), a finding consistent with the basal hyperinsulinaemia seen in these mice (Fig. 2b). However, while insulin increased phosphorylation (Ser⁴⁷³) of Akt in the livers of control mice, this was not observed in *Il6*^{-/-} mice (Fig. 4f). Accordingly, insulin-stimulated phosphorylation (Ser⁴⁷³) of Akt was lower in the liver of *Il6*^{-/-} mice than in that of control animals (Fig. 4f).

High fat feeding in Il6^{-/-} mice results in hepatic insulin resistance, in the absence of exacerbated obesity and ectopic lipid accumulation in the liver To determine the effect of global IL-6 deletion in the context of diet-induced obesity and insulin resistance, we placed 8-week-old *Il6*^{-/-} and control mice on a HFD for 12 weeks. The obesity phenotype observed on a standard chow diet was not exacerbated by a HFD, with *Il6*^{-/-} and control mice: (1) displaying similar fat mass, lean mass and total body mass (Fig. 5a); (2) consuming similar amounts of food (Fig. 5b); and (3) being undistinguishable with respect to $\dot{V}O_2$ (Fig. 5c), movement (Fig. 5d) and respiratory exchange ratio (Fig. 5e), and generally having similar levels of triacylglycerol and diacylglycerol in liver and skeletal muscle (ESM Fig. 4a–d). Despite these observations after 12 weeks on HFD, the *Il6*^{-/-} mice displayed fasting hyperinsulinaemia (Fig. 6a), insulin intolerance (Fig. 6b, c) and reduced insulin signalling in the liver as measured by phosphorylation (Ser⁴⁷³) of Akt (Fig. 6d). Intriguingly, although the degree of hepato-steatosis as measured by triacylglycerol, diacylglycerol and ceramide accumulation was not different when comparing *Il6*^{-/-} with control mice, histological examination by haematoxylin and eosin staining revealed evidence of liver damage, as indicated by dilated vasculature and inflammatory cell infiltration in *Il6*^{-/-} mice. In contrast, in control mice, there were large areas of intact parenchyma, which is indicative of healthy hepatocytes, and evidence of numerous bi-nucleated

Fig. 4 *Il6*^{-/-} mice display liver inflammation and liver insulin resistance. **a** Serum ALT. Representative immunoblots and quantification by mouse type of: **b** total and phosphorylated (Thr¹⁸³/Tyr¹⁸⁵) JNK; phosphorylated IKK α (Ser¹⁸⁰)/IKK β (Ser¹⁸¹) and β -actin (**c**); pre- and pro-TNF α and β -actin (**d**); PKC θ protein levels (**e**); and total and phosphorylated (Ser⁴⁷³) Akt basal and insulin-stimulated (**f**). All measurements in liver samples obtained from control (black bars) and *Il6*^{-/-} (grey bars) mice at 20 weeks of age. Mice were maintained on a standard chow diet. Data expressed as mean \pm SEM, $n=8$ animals per group for (**b**), $n=4-7$ animals per group (**a**, **c-f**); * $p<0.05$ for difference



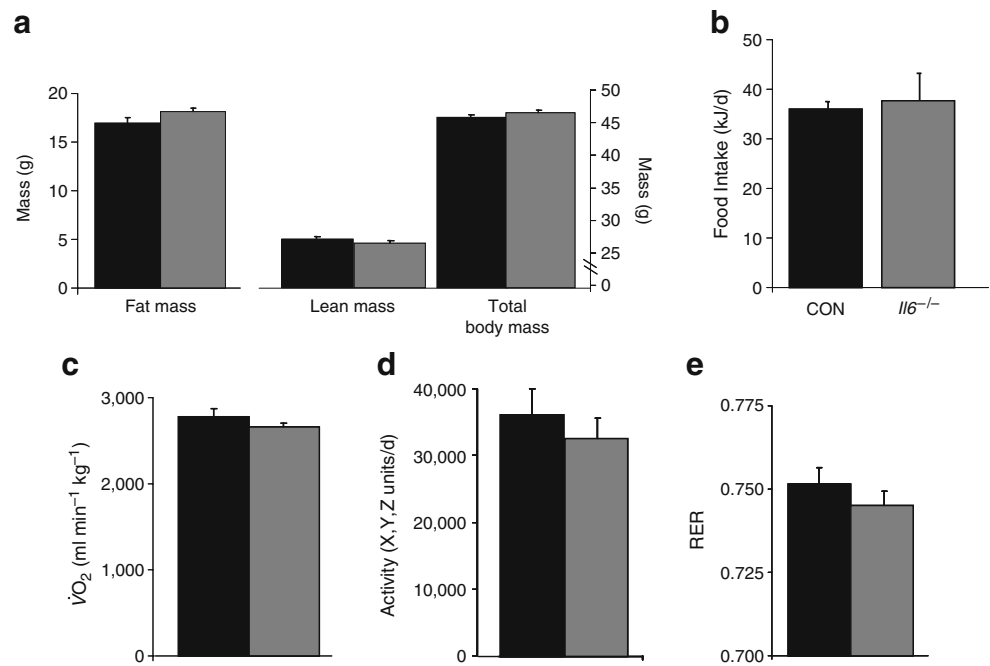
hepatocytes indicative of liver regeneration (Fig. 6e). In addition, ALT levels were markedly elevated in *Il6*^{-/-} mice compared with control on HFD (Fig. 6f).

Genes associated with the tricarboxylic acid cycle, electron transport chain and oxidative phosphorylation are coordinately reduced in livers from HFD-fed Il6^{-/-} mice *Il6*^{-/-} mice displayed liver insulin resistance, and liver inflammation and damage, despite having a similar degree of adiposity and liver lipid accumulation to that seen in control mice. Since we were unable to determine the mechanism for this phenotype, we next performed microarray analysis on liver samples from animals fed the HFD. We employed GSEA, a computational method that determines whether an a priori defined set of genes shows statistically significant, concordant differences between two biological states. These analyses revealed that

four such defined sets of genes were downregulated ($p<0.05$) in livers from HFD *Il6*^{-/-} compared with control mice. These included ‘Nadler Obesity Hyperglycaemia’ [29] (ESM Fig. 5). This defined gene set included genes involved in signal transduction and energy metabolism, as well as genes not previously examined in the context of diabetes. Nadler et al. [29] demonstrated that a decrease in expression of this gene set was associated with obesity and hyperglycaemia. In addition, the other related sets of genes that were coordinately downregulated were genes associated with the tricarboxylic acid cycle (Fig. 7a), electron transport chain (Fig. 7b) and oxidative phosphorylation (Fig. 7c).

Indices of oxidative phosphorylation are reduced in livers from HFD-fed Il6^{-/-} mice Given the coordinate down-regulation of genes associated with the tricarboxylic acid

Fig. 5 *Il6*^{-/-} mice possess normal body weight, fat mass and behaviour when fed a HFD. Fat mass, lean mass and total body mass (a), food intake (b), $\dot{V}O_2$ (c) and activity (d), and respiratory exchange ratio (RER) (e) obtained from control (CON; black bars) and *Il6*^{-/-} (grey bars) mice at 20 weeks of age, after administration of a HFD from 8 weeks. Data expressed as mean \pm SEM, $n=15-17$ animals per group for (a), $n=4-6$ animals per group (b-e)



cycle, electron transport chain and oxidative phosphorylation, we next examined other indices of mitochondrial function and/or capacity. Citrate synthase and β -HAD are key enzymes involved in mitochondrial function. While citrate synthase was not different (data not shown), β -HAD was reduced in livers of HFD *Il6*^{-/-} compared with control

mice (Fig. 8a). In addition, the mRNA abundance (measured by realtime RT-PCR) of carnitine palmitoyltransferase-1, the enzyme that controls entry of long-chain fatty acyl CoA into mitochondria, was also markedly reduced in *Il6*^{-/-} mice (Fig. 8b). Finally, we measured levels of mitochondrial respiratory chain proteins in the livers of HFD *Il6*^{-/-} and

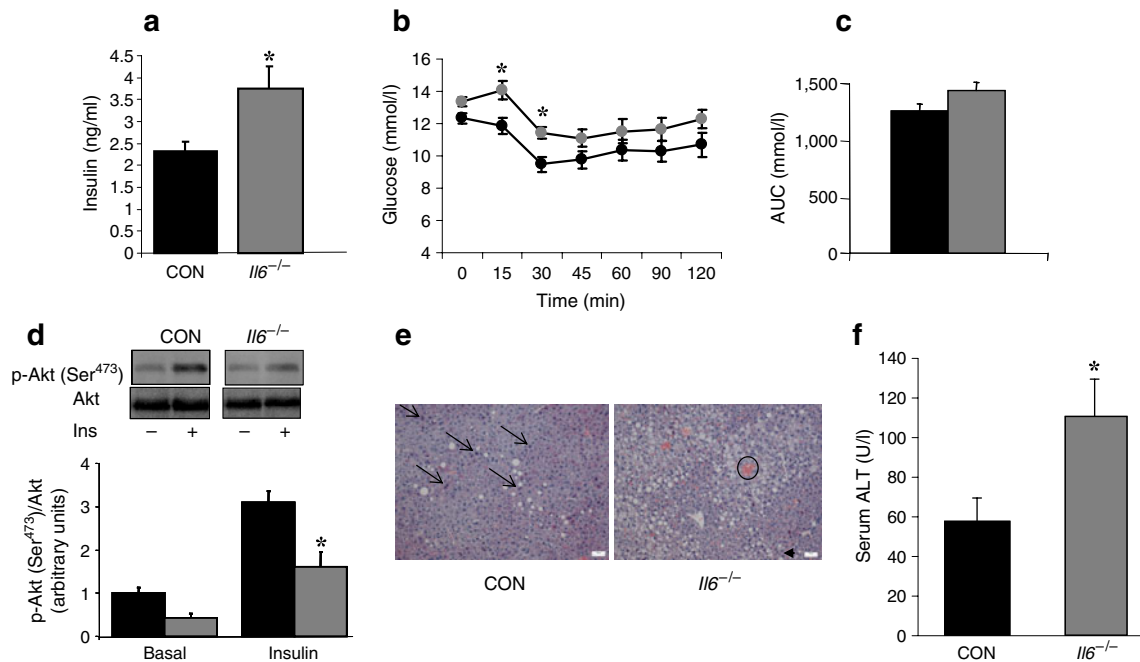


Fig. 6 *Il6*^{-/-} mice exhibit liver inflammation and insulin resistance when fed a HFD. Plasma insulin (a), insulin tolerance (b) with AUC (c), total and phosphorylated (Ser⁴⁷³) Akt in liver (d), liver histology (e) and serum ALT (f) obtained from control (CON; black bars and/or circles) and *Il6*^{-/-} (grey bars and/or circles) mice at 20 weeks of age,

after administration of a HFD from 8 weeks. e Arrows pointing to right, bi-nucleated hepatocytes; circle, dilated vasculature; arrow pointing to left, inflammatory cell infiltration. Data expressed as mean \pm SEM, $n=4-6$ animals per group (a, d-f), $n=15-17$ animals per group (b); * $p<0.05$ for difference

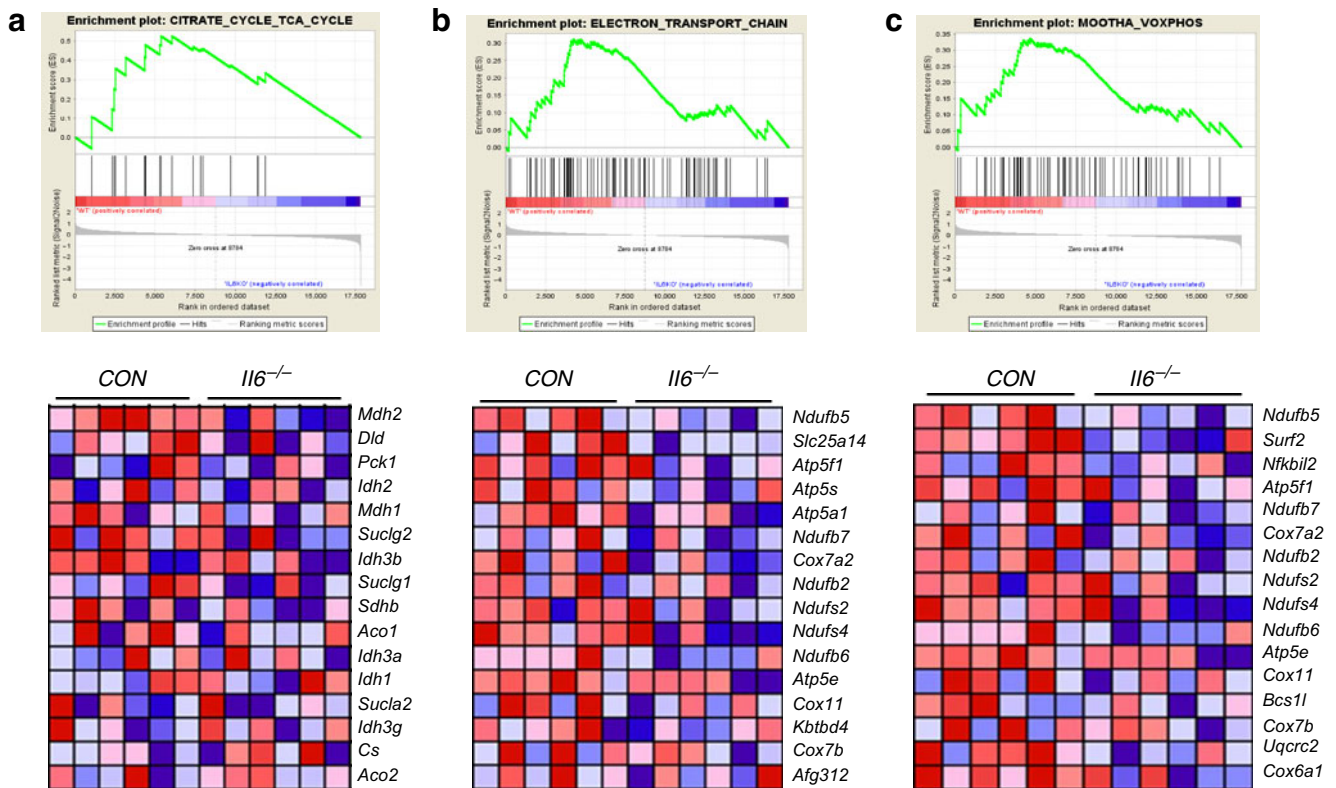


Fig. 7 *Il6*^{-/-} mice exhibit defective mitochondrial gene expression when fed a HFD. **a** Enrichment plots and heat maps for genes associated with the citric acid cycle, **b** electron transport chain and **c** oxidative phosphorylation in liver as determined by GSEA. Red,

increased expression; blue, decreased expression. Liver was obtained from control and *Il6*^{-/-} mice at 20 weeks of age, after administration of a HFD from 8 weeks. *n*=6 animals per group

control mice. Although there were no differences in Complex I and Complex V respiratory chain proteins, levels of Complex II, Complex II,III and Complex IV subunit I were markedly reduced in *Il6*^{-/-} compared with control mice (Fig. 8c, d).

Discussion

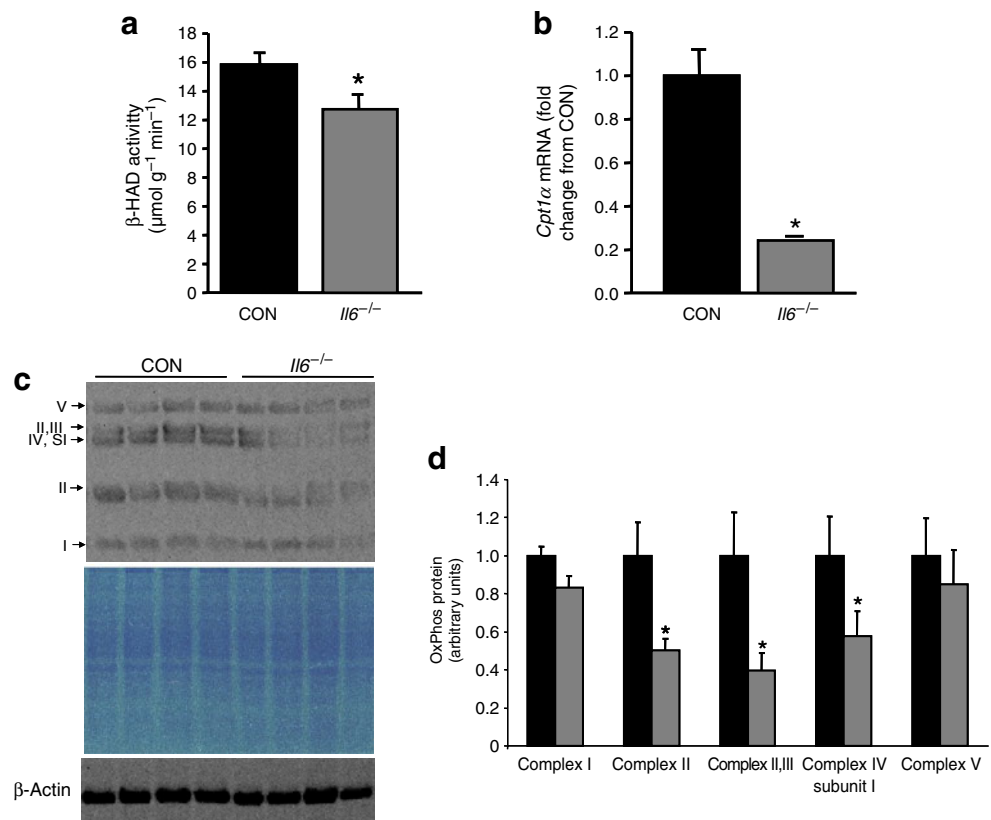
The role of IL-6 in the development of obesity and insulin resistance remains unresolved [30]. Here we provide clear evidence that mice with global deletion of IL-6 not only develop obesity, but also hepatosteatosis, liver inflammation and impaired whole-body insulin sensitivity. Moreover, when fed a HFD, the inflammatory phenotype in the liver and whole-body insulin resistance remained prevalent in *Il6*^{-/-} mice, despite equivalent fat mass and ectopic lipid levels in liver relative to control animals. These data demonstrate that a lack of IL-6 leads to liver inflammation and insulin resistance, irrespective of adiposity, demonstrating that IL-6 is required for protection against hepatic inflammation and insulin resistance when mice are challenged with a HFD.

While our model demonstrates that IL-6 is necessary to prevent hepatic inflammation, it is generally accepted that

IL-6 is pro-inflammatory in human disease. Indeed, tocilizumab, the first IL-6 receptor-inhibiting monoclonal antibody, has recently been approved for the treatment of adult patients with moderate to severe rheumatoid arthritis and other inflammatory disorders. It should be noted, however, that rheumatoid arthritis patients treated with tocilizumab exhibit weight gain and hyperlipidaemia, as reviewed by Febbraio et al. [31], results that are consistent with the present data set. It should also be noted that IL-6 can also be anti-inflammatory in humans, as recombinant human IL-6 infusion prevents endotoxin-induced TNF- α production [32]. Moreover, in a recent paper, Fosgerau et al. [33] reported that humans can produce IL-6 autoantibodies. Importantly, the prevalence of circulating high-affinity neutralising IL-6 autoantibodies was 2.5 times higher in patients with type 2 diabetes than in control patients. Hence, while IL-6 is clearly pro-inflammatory in a range of diseases such as rheumatoid arthritis, completely blocking IL-6 signalling can result in weight gain and hyperlipidaemia.

Our observation that *Il6*^{-/-} mice become obese is consistent with some [16], but not all [17] previous reports. Recently, another team demonstrated that human IL-6 transgenic mice with sustained elevated circulating IL-6 display enhanced central leptin action and improved

Fig. 8 *Il6*^{-/-} mice display defective mitochondrial function when fed a HFD. **a** Maximal activity of β -HAD and **(b)** carnitine palmitoyl-transferase 1 mRNA expression as measured by real-time RT-PCR in liver. **c** Representative immunoblot of oxidative phosphorylation (OxPhos) protein Complexes I to V as labelled, brilliant blue stain for total protein and blot of β -actin, quantified **(d)** in liver obtained from control (CON; black bars) and *Il6*^{-/-} (grey bars) mice at 20 weeks of age, after administration of a HFD from 8 weeks. Data expressed as mean \pm SEM, $n=6-8$ animals per group; * $p<0.05$ for difference



nutrient homeostasis leading to protection from diet-induced obesity [15]. These recent data [15] are consistent with the notion that IL-6-deficient mice would display an obese phenotype, since chronic IL-6 prevents obesity due to enhanced leptin action. In the present study, however, we were unable to consistently measure any increase in feeding or decrease in energy expenditure in *Il6*^{-/-} mice that could explain their development of obesity. However, although the mice increased their body weight by 15% over the 20 weeks (Fig. 1a), the overall difference in fat mass was 3 g (Fig. 1b). This would equate to an increase of 0.02 g fat or 0.84 kJ/day. The daily energy expenditure of a mouse has been estimated to be 42 kJ/day [34]. Consequently, a 2% difference in daily energy expenditure would be sufficient to result in the increased body weight, but unlikely to be detected with available techniques. Similar problems have been encountered in other mouse models of obesity [34, 35].

While the role of IL-6 in whole-body insulin resistance is unclear, it is generally accepted that excessive circulating IL-6 causes hepatic insulin resistance [30]. This conclusion is based on several observations demonstrating that exogenous administration of IL-6 impairs insulin signal transduction in the liver in vitro [36, 37] and in vivo [13]. In addition, IL-6-neutralising antibodies have been shown to reverse hepatic insulin resistance in mice [38, 39], while transient overproduction of IL-6 in skeletal muscle by in

vivo electroporation resulted in liver inflammation [40]. In contrast with these studies, our data demonstrate that an absence of IL-6 in otherwise healthy mice leads to liver inflammation. It is well known that non-alcoholic fatty liver disease is a hallmark precursor of non-alcoholic steatohepatitis. In the present study, the absence of IL-6 led to liver inflammation which was independent of liver lipid accumulation. The serum ALT concentration in the chow-fed *Il6*^{-/-} mice was ~60 U/l (Fig. 4a), which was approximately equal to that observed in the HFD-fed control mice (Fig. 6f). However, the liver triacylglycerol and diacylglycerol species were around three- to five fold higher in the HFD-fed control mice than in the chow-fed *Il6*^{-/-} mice. These data therefore argue that an absence of IL-6 signalling in the liver leads to liver inflammation and damage, irrespective of liver lipid content, reiterating the importance of monitoring for liver complications associated with human IL-6 receptor blockade therapy.

The present data are in accordance with some [18, 41], but not all [17, 42] previous studies in IL-6-deficient mice. It should be noted that in the more recent study [42], the IL-6-deficient mice did not develop obesity. The reasons for these discrepancies are not readily apparent but, could be due to differences between C57BL/6 substrains, due to genetic drift. In the present study, we backcrossed our *Il6*^{-/-} mice on to a C57BL/6 background at least nine times to reduce genetic heterogeneity and compared *Il6*^{-/-} and *Il6*^{+/+}

from the same litters in all circumstances. In addition, differences in results when comparing *Il6*^{-/-} studies could be due to environmental differences between animal facilities. As IL-6 is a component of the immune system, one possibility is differences in exposure to pathogenic agents. Accordingly, in the present study, we were very careful to keep our mice pathogen-free. To this end, we analysed the digestive tract for a range of bacterial strains such as *Clostridium piliforme*, *Salmonella enteritidis* and *Helicobacter*. These tests were all negative in both strains. *Helicobacter*, in addition, was not detected in faeces and faecal lipid content was not different between strains.

In the past decade, it has become apparent that insulin resistance is associated with impaired mitochondrial function in skeletal muscle [43]. Two DNA microarray studies found a coordinated reduction in *PGC-1 α* gene expression in the skeletal muscle of type 2 diabetic patients [21, 44] and non-diabetic participants with a family history of diabetes [44]. In addition, studies using nuclear magnetic resonance spectroscopy have demonstrated that mitochondrial function in skeletal muscle plays an important role in the pathogenesis of type 2 diabetes [45] and in young lean insulin-resistant offspring of parents with type 2 diabetes [46]. Although less well studied, there is also evidence that defective mitochondrial function in liver is associated with insulin resistance in rodent models of insulin resistance [47]. In addition, mitochondrial abnormalities such as depletion of mitochondrial DNA, decreased activity of respiratory chain complexes, and impaired mitochondrial β -oxidation and mitochondrial DNA complexes have been observed in patients with non-alcoholic fatty liver disease [48, 49]. IL-6 treatment has previously been shown to decrease oxidative injury after 87% hepatectomy in mice [50]. Using GSEA, we demonstrated here that global deletion of IL-6 in mice resulted in a co-ordinate down-regulation of genes associated with the tricarboxylic acid cycle, the electron transport chain and oxidative phosphorylation. Consistent with these findings, we also observed a decrease in the maximal activity of β -HAD and reduced expression of respiratory Complexes II, III and IV (subunit I) in *Il6*^{-/-} mice relative to control when fed a HFD. Together, these data suggest that when these mice are metabolically challenged with a HFD, IL-6 deficiency is associated with altered mitochondrial function and insulin resistance in the liver, possibly via elimination of reactive oxygen species.

In conclusion, we demonstrated that global deletion of IL-6 in mice results in maturity-onset obesity, hepatosteatosis, liver inflammation and insulin resistance when animals are maintained on a standard chow diet. Importantly, when *Il6*^{-/-} mice are challenged by high-fat feeding, inflammation and insulin resistance remain, against a setting of equivalent fat mass and ectopic lipid levels in liver relative to control animals. Thus our data suggest that

a lack of IL-6 exacerbates liver inflammation and insulin resistance.

Acknowledgements This study was funded by a project grant from the National Health and Medical Research Council of Australia (NHMRC Project Grant 526606). The support of the BakerIDI Lipodomics, Genomics and Mouse Metabolic Phenotyping Core Facilities is gratefully acknowledged. J. B. Jowett, V. B. Matthews and C. R. Bruce are Career Development Fellows, P. J. Meikle and M. J. Watt are Senior Research Fellows, and M. A. Febbraio is a Principal Research Fellow of the NHMRC. We thank I. Haviv for his helpful discussions about the GSEA.

Duality of interest The authors declare that there is no duality of interest associated with this manuscript.

References

- Hotamisligil GS (2006) Inflammation and metabolic disorders. *Nature* 444:860–867
- Carey AL, Bruce CR, Sacchetti M et al (2004) Interleukin-6 and tumor necrosis factor- α are not increased in patients with type 2 diabetes: evidence that plasma interleukin-6 is related to fat mass and not insulin responsiveness. *Diabetologia* 47:1029–1037
- Lazar MA (2005) How obesity causes diabetes: not a tall tale. *Science* 307:373–375
- Pedersen BK, Febbraio MA (2008) Muscle as an endocrine organ: focus on muscle-derived interleukin-6. *Physiol Rev* 88:1379–1406
- Al-Khalili L, Bouzakri K, Glund S, Lonnqvist F, Koistinen HA, Krook A (2006) Signaling specificity of interleukin-6 action on glucose and lipid metabolism in skeletal muscle. *Mol Endocrinol* 20:3364–3375
- Bruce CR, Dyck DJ (2004) Cytokine regulation of skeletal muscle fatty acid metabolism: effect of interleukin-6 and tumor necrosis factor- α . *Am J Physiol Endocrinol Metab* 287:E616–E621
- Carey AL, Steinberg GR, Macaulay SL et al (2006) Interleukin-6 increases insulin-stimulated glucose disposal in humans and glucose uptake and fatty acid oxidation in vitro via AMP-activated protein kinase. *Diabetes* 55:2688–2697
- Glund S, Deshmukh A, Long YC et al (2007) Interleukin-6 directly increases glucose metabolism in resting human skeletal muscle. *Diabetes* 56:1630–1637
- Petersen EW, Carey AL, Sacchetti M et al (2005) Acute IL-6 treatment increases fatty acid turnover in elderly humans in vivo and in tissue culture in vitro. *Am J Physiol Endocrinol Metab* 288: E155–E162
- Rotter Sopasakis V, Larsson BM, Johansson A, Holmang A, Smith U (2004) Short-term infusion of interleukin-6 does not induce insulin resistance in vivo or impair insulin signalling in rats. *Diabetologia* 47:1879–1887
- Yuen DY, Dwyer RM, Matthews VB et al (2009) Interleukin-6 attenuates insulin-mediated increases in endothelial cell signaling but augments skeletal muscle insulin action via differential effects on tumor necrosis factor- α expression. *Diabetes* 58:1086–1095
- Kim HJ, Higashimori T, Park SY et al (2004) Differential effects of interleukin-6 and 10 on skeletal muscle and liver insulin action in vivo. *Diabetes* 53:1060–1067
- Klover PJ, Zimmers TA, Koniaris LG, Mooney RA (2003) Chronic exposure to interleukin-6 causes hepatic insulin resistance in mice. *Diabetes* 52:2784–2789
- Holmes AG, Mesa JL, Neill BA et al (2008) Prolonged interleukin-6 administration enhances glucose tolerance and

- increases skeletal muscle PPARalpha and UCP2 expression in rats. *J Endocrinol* 198:367–374
15. Sadagurski M, Norquay L, Farhang J, D'Aquino K, Copps K, White MF (2010) Human IL6 enhances leptin action in mice. *Diabetologia* 53:525–535
 16. Wallenius V, Wallenius K, Ahren B et al (2002) Interleukin-6-deficient mice develop mature-onset obesity. *Nat Med* 8:75–79
 17. Di Gregorio GB, Hensley L, Lu T, Ranganathan G, Kern PA (2004) Lipid and carbohydrate metabolism in mice with a targeted mutation in the IL-6 gene: absence of development of age-related obesity. *Am J Physiol Endocrinol Metab* 287:E182–E187
 18. Kopf M, Baumann H, Freer G et al (1994) Impaired immune and acute-phase responses in interleukin-6-deficient mice. *Nature* 368:339–342
 19. Chung J, Nguyen AK, Henstridge DC et al (2008) HSP72 protects against obesity-induced insulin resistance. *Proc Natl Acad Sci USA* 105:1739–1744
 20. Watt MJ, Dzamko N, Thomas WG et al (2006) CNTF reverses obesity-induced insulin resistance by activating skeletal muscle AMPK. *Nat Med* 12:541–548
 21. Mootha VK, Lindgren CM, Eriksson KF et al (2003) PGC-1alpha-responsive genes involved in oxidative phosphorylation are coordinately downregulated in human diabetes. *Nat Genet* 34:267–273
 22. Subramanian A, Tamayo P, Mootha VK et al (2005) Gene set enrichment analysis: a knowledge-based approach for interpreting genome-wide expression profiles. *Proc Natl Acad Sci USA* 102:15545–15550
 23. Bruce CR, Hoy AJ, Turner N et al (2009) Overexpression of carnitine palmitoyltransferase-1 in skeletal muscle is sufficient to enhance fatty acid oxidation and improve high-fat diet-induced insulin resistance. *Diabetes* 58:550–558
 24. Solinas G, Naugler W, Galimi F, Lee MS, Karin M (2006) Saturated fatty acids inhibit induction of insulin gene transcription by JNK-mediated phosphorylation of insulin-receptor substrates. *Proc Natl Acad Sci USA* 103:16454–16459
 25. Yuan M, Konstantopoulos N, Lee J et al (2001) Reversal of obesity- and diet-induced insulin resistance with salicylates or targeted disruption of Ikkbeta. *Science* 293:1673–1677
 26. Hirosumi J, Tuncman G, Chang L et al (2002) A central role for JNK in obesity and insulin resistance. *Nature* 420:333–336
 27. Lam TK, Yoshii H, Haber CA et al (2002) Free fatty acid-induced hepatic insulin resistance: a potential role for protein kinase C-delta. *Am J Physiol Endocrinol Metab* 283:E682–E691
 28. Kim JK, Fillmore JJ, Sunshine MJ et al (2004) PKC-theta knockout mice are protected from fat-induced insulin resistance. *J Clin Invest* 114:823–827
 29. Nadler ST, Stoehr JP, Schueler KL, Tanimoto G, Yandell BS, Attie AD (2000) The expression of adipogenic genes is decreased in obesity and diabetes mellitus. *Proc Natl Acad Sci USA* 97:11371–11376
 30. Feve B, Bastard JP (2009) The role of interleukins in insulin resistance and type 2 diabetes mellitus. *Nat Rev Endocrinol* 5:305–311
 31. Febbraio MA, Rose-John S, Pedersen BK (2010) Is interleukin-6 receptor blockade the Holy Grail for inflammatory diseases? *Clin Pharmacol Ther* 87:396–398
 32. Starkie R, Ostrowski SR, Jauffred S, Febbraio M, Pedersen BK (2003) Exercise and IL-6 infusion inhibit endotoxin-induced TNF-alpha production in humans. *FASEB J* 17:884–886
 33. Fosgerau K, Galle P, Hansen T et al (2010) Interleukin-6 autoantibodies are involved in the pathogenesis of a subset of type 2 diabetes. *J Endocrinol* 204:265–273
 34. Tschop M, Smiley DL, Heiman ML (2000) Ghrelin induces adiposity in rodents. *Nature* 407:908–913
 35. Garcia MC, Wernstedt I, Berndtsson A et al (2006) Mature-onset obesity in interleukin-1 receptor I knockout mice. *Diabetes* 55:1205–1213
 36. Henkel J, Neuschaefer-Rube F, Pathe-Neuschaefer-Rube A, Puschel GP (2009) Aggravation by prostaglandin E2 of interleukin-6-dependent insulin resistance in hepatocytes. *Hepatology* 50:781–790
 37. Senn JJ, Klover PJ, Nowak IA, Mooney RA (2002) Interleukin-6 induces cellular insulin resistance in hepatocytes. *Diabetes* 51:3391–3399
 38. Cai D, Yuan M, Frantz DF et al (2005) Local and systemic insulin resistance resulting from hepatic activation of IKK-beta and NF-kappaB. *Nat Med* 11:183–190
 39. Klover PJ, Clementi AH, Mooney RA (2005) Interleukin-6 depletion selectively improves hepatic insulin action in obesity. *Endocrinology* 146:3417–3427
 40. Franckhauser S, Elias I, Rotter Sopasakis V et al (2008) Overexpression of Il6 leads to hyperinsulinaemia, liver inflammation and reduced body weight in mice. *Diabetologia* 51:1306–1316
 41. Cressman DE, Greenbaum LE, DeAngelis RA et al (1996) Liver failure and defective hepatocyte regeneration in interleukin-6-deficient mice. *Science* 274:1379–1383
 42. Park EJ, Lee JH, Yu GY et al (2010) Dietary and genetic obesity promote liver inflammation and tumorigenesis by enhancing IL-6 and TNF expression. *Cell* 140:197–208
 43. Morino K, Petersen KF, Shulman GI (2006) Molecular mechanisms of insulin resistance in humans and their potential links with mitochondrial dysfunction. *Diabetes* 55(Suppl 2):S9–S15
 44. Patti ME, Butte AJ, Crunkhorn S et al (2003) Coordinated reduction of genes of oxidative metabolism in humans with insulin resistance and diabetes: potential role of PGC1 and NRF1. *Proc Natl Acad Sci USA* 100:8466–8471
 45. Petersen KF, Befroy D, Dufour S et al (2003) Mitochondrial dysfunction in the elderly: possible role in insulin resistance. *Science* 300:1140–1142
 46. Petersen KF, Dufour S, Befroy D, Garcia R, Shulman GI (2004) Impaired mitochondrial activity in the insulin-resistant offspring of patients with type 2 diabetes. *N Engl J Med* 350:664–671
 47. Kim JA, Wei Y, Sowers JR (2008) Role of mitochondrial dysfunction in insulin resistance. *Circ Res* 102:401–414
 48. Perez-Carreras M, Del Hoyo P, Martin MA et al (2003) Defective hepatic mitochondrial respiratory chain in patients with nonalcoholic steatohepatitis. *Hepatology* 38:999–1007
 49. Pessayre D, Fromenty B (2005) NASH: a mitochondrial disease. *J Hepatol* 42:928–940
 50. Jin X, Zhang Z, Beer-Stolz D, Zimmers TA, Koniaris LG (2007) Interleukin-6 inhibits oxidative injury and necrosis after extreme liver resection. *Hepatology* 46:802–812